MULTIBODY DYNAMICS 2007, ECCOMAS Thematic Conference
C.L. Bottasso, P. Masarati, L. Trainelli (eds.)
Milano, Italy, 25–28 June 2007

ORTHOGONAL PROJECTION METHODS FOR THE KINEMATIC DATA CONSISTENCY OF BIOMECHANICAL SYSTEMS

F.J. Alonso[⋆], J. Cuadrado[†], J.M. Del Castillo[⋆] and P. Pintado[‡]

[⋆]Departamento de Ingeniería Mecánica, Energética y de los Materiales
Universidad de Extremadura, Avda. de Elvas s/n, 06071 Badajoz, Spain
e-mails: fjas@unex.es, delcasti@unex.es

[†]Departamento de Ingeniería Industrial II
Universidad de La Coruña, Mendizábal s/n, 15403 Ferrol, Spain
e-mail: javicuad@cdf.udc.es

[‡]Departamento de Mecánica Aplicada
Universidad de Castilla La Mancha, Camilo José Cela s/n, 13071 Ciudad Real, Spain
e-mail: Publio.Pintado@uclm.es

Keywords: Biomechanics, Skin Motion, Kinematic Consistency, Orthogonal Projection Methods, Inverse Dynamic Analysis.

Abstract. *The estimation of the skeletal motion obtained from marker-based motion capture systems is known to be affected by significant errors caused by skin motion artifact, i.e. the motion of the skin with respect to the underlying bone. The skin motion artifact produces violations of the kinematic constraint equations of the multibody system. This violation is called kinematic data inconsistency and is regarded as one of the most critical sources of error in human movement analysis. A systematic multibody procedure based on orthogonal projection of the position, velocity and acceleration solution to ensure the kinematic data consistency in the context of the analysis of biomechanical systems is presented. The procedure corrects the marker positions and the intersegmental angles simultaneously. The raw data differentiation problem is solved by applying a smoothing technique based on singular spectrum analysis. Several kinematic signals that include computer generated data of a four-bar mechanism and experimental acquired data from a normal subject performing three different physical activities were processed using the smoothing procedure and the projection methods to study its performance.*

1 INTRODUCTION

Biomechanics studies, namely Kinematic and Inverse Dynamics Analysis (IDA), use non-invasive three dimensional (3-D) motion analysis using stereophotogrammetry to estimate skeletal motion. This technique reconstructs the 3D position of a retroreflective marker set located on the skin surface of the human body.

The estimation of the skeletal motion obtained from marker-based motion capture systems is known to be affected by significant errors caused by skin motion artifact [1, 2], i.e. the motion of the skin with respect to the underlying bone, and due to the amplification of high-frequency low-amplitude noise introduced by the motion capture system when the raw displacement signals are differentiated to obtain velocities and accelerations.

To avoid raw data amplification during differentiation, the acquired displacement signals are smoothed prior to differentiation. It is important to note that the raw data smoothing procedure does not eliminate the skin motion artifact [1–4]. This is because the skin motion artifact has a frequency content near to the actual bone movement and it is therefore very difficult to distinguish between the two by means of any filtering technique [2]. Moreover, the smoothing procedure does not ensure the kinematic data consistency with the biomechanical model because the kinematic constraint equations are not necessarily satisfied [5].

2 KINEMATIC DATA CONSISTENCY

The skin motion artifact affects the kinematics of the multibody system, producing violations of the kinematic constraint equations. For example, the length of each body segment does not remains constant during the simulation [4] (see Fig. 1). This violation is called kinematic data inconsistency and is regarded as one of the most critical sources of error in human movement analysis [5]. Namely, this inconsistency produces spurious reaction forces and driver moments when IDA is performed.

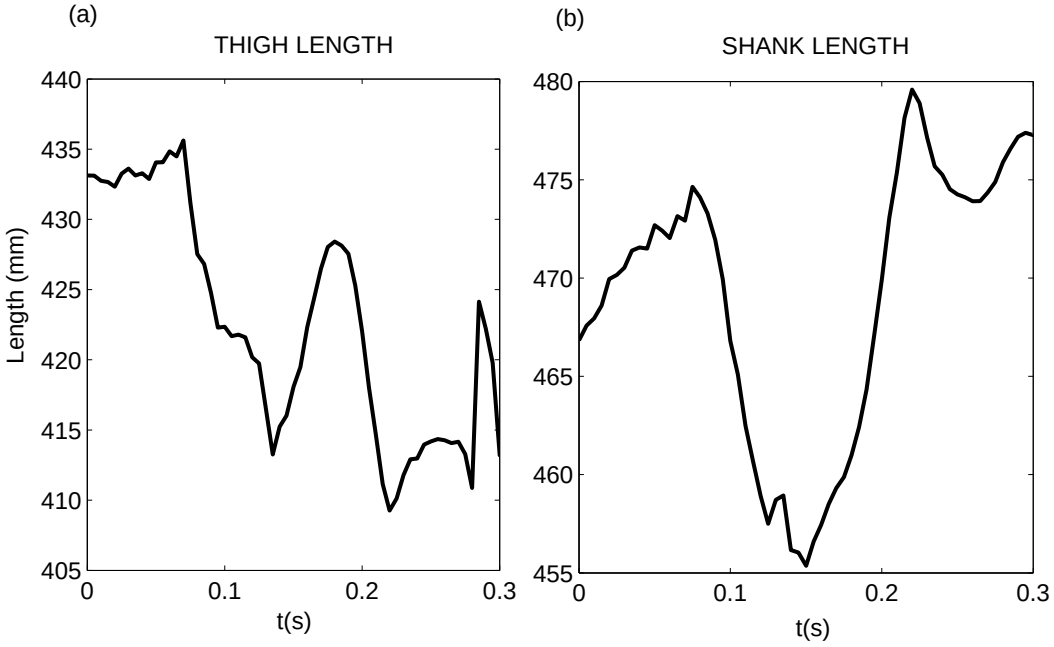

Figure 1: Thigh length (a) and shank length (b) during the impact phase of a drop landing from a height of 0.5 m.

In this work, we correct the displacement signals in order to satisfy the kinematic multibody equations. A mechanical system is consistent with the acquired kinematic data when the constraint equations and their time derivatives are satisfied [5–7]. Techniques designed to compensate the effects of the skin motion artifact can be divided up into those which model the skin surface and those which include kinematic constraints equations of the multibody model [2].

Silva and Ambrósio [5] applied a systematic procedure using a multibody formalism to ensure kinematic data consistency. They use the non-consistent $\mathbf{q}^*$ positions as an initial guess to the Newton-Raphson procedure to obtain consistent positions $\mathbf{q}$:

$$\mathbf{\Phi_q}(\mathbf{q}_i)\mathbf{\Delta q}_i = -\mathbf{\Phi}(\mathbf{q}_i) \tag{1}$$

Where $\mathbf{\Delta q}_i = \mathbf{q} - \mathbf{q}_i$ is the generalized coordinates correction at iteration i. Consistent velocities $\dot{\mathbf{q}}$ and accelerations $\ddot{\mathbf{q}}$ are obtained by solving velocity and acceleration equations of the multibody system:

$$\mathbf{\Phi_q}(\mathbf{q})\dot{\mathbf{q}} = \mathbf{0} \tag{2}$$

$$\mathbf{\Phi_q}(\mathbf{q})\ddot{\mathbf{q}} = -\dot{\mathbf{\Phi}}_\mathbf{q}\dot{\mathbf{q}} \tag{3}$$

This procedure produces reasonable good results [5]. Nevertheless, the biomechanical model is driven by the angular histories calculated from the inconsistent input data, which are not the true angular histories.

To overcome the calculation of the intersegmental angles from inconsistent data, this work proposes the simultaneous correction of the natural coordinates and intersegmental angles performing an orthogonal projection of the position solution to the constraint manifold, in order to obtain a new set of positions $\mathbf{q}$ that satisfies $\mathbf{\Phi} = \mathbf{0}$. This scheme projects the subset of natural coordinates measured with the motion capture system and calculates the angular histories from the consistent positions. The projection can be obtained by the solution of the following constrained minimization problem [6]:

$$min_\mathbf{q} V = \frac{1}{2}(\mathbf{q} - \mathbf{q}^*)^T\mathbf{W}(\mathbf{q} - \mathbf{q}^*) \quad s.t. \quad \mathbf{\Phi} = \mathbf{0} \tag{4}$$

Where $\mathbf{W}$ is a weighting matrix. Different weighting factors can be assigned to each natural coordinate to reflect the average degree of skin movement artifact associated to each coordinate. For example, skin movement artifact on the thigh is larger than on the shank [8, 9].

Using an augmented Lagrangian method to minimize the above function [6], the following iterative scheme to calculate the consistent data positions $\mathbf{q}$ is obtained:

$$[\mathbf{W} + \mathbf{\Phi_q}^T\alpha\mathbf{\Phi_q}]\mathbf{\Delta q}_{i+1} = -\mathbf{W}\mathbf{\Delta q}_i - \mathbf{\Phi_q}^T\alpha\mathbf{\Phi} \tag{5}$$

Where $\mathbf{\Delta q}_{i+1}$ and $\mathbf{\Delta q}_i$ are the position data corrections and the subscripts indicate the iteration number. Equation (5) can be solved iteratively until $||\mathbf{\Delta q}|| < \epsilon$, where ϵ is a user specified tolerance. The value of the penalty factor α only affects the convergence rate. Bayo et al. [6] recommend penalty factors ranging from 10^5 to 10^7 to obtain a good convergence rate.

In order to obtain consistent velocities $\dot{\mathbf{q}}$ again we perform an orthogonal projection of the velocities $\dot{\mathbf{q}}^*$ calculated using finite differences to the velocity constraint manifold. This can be achieved by the solution of the linear equation:

$$[\mathbf{W} + \mathbf{\Phi_q}^T\alpha\mathbf{\Phi_q}]\dot{\mathbf{q}} = \mathbf{W}\dot{\mathbf{q}}^* \tag{6}$$

To obtain consistent accelerations the projection of the accelerations $\ddot{\mathbf{q}}^*$ calculated using finite differences onto the constraint manifold can be obtained trough the solution of the following equation:

$$[\mathbf{W} + \mathbf{\Phi_q}^T \alpha \mathbf{\Phi_q}]\ddot{\mathbf{q}} = \mathbf{W}\ddot{\mathbf{q}}^* - \mathbf{\Phi_q}^T \alpha \dot{\mathbf{\Phi}}_\mathbf{q} \dot{\mathbf{q}} \tag{7}$$

3 DATA SMOOTHING: SINGULAR SPECTRUM ANALYSIS

The motion capture systems used in biomechanical analysis introduce systematic and random measurement errors that appear in the form of high-frequency noise in the recorded displacement signals. The noise is amplified when differentiating the displacements to obtain velocities and accelerations [8–18]. This problem is well known to be ill-posed in the sense that a small error in position data can induce a large error in the approximate derivatives and could cause unacceptable errors in the Inverse Dynamic Analysis (IDA) of biomechanical systems [14–15]. To avoid this phenomenon it is necessary to filter the displacement signal prior to differentiation.

The filtering of displacement signals to obtain noiseless velocities and accelerations has been extensively treated in the literature. Traditional filtering techniques include digital Butterworth filters, splines, and filters based on spectral analysis [8–11]. Nonetheless, traditional filtering methods are not suited for smoothing non-stationary signals. This drawback is particularly problematic in biomechanical analysis since physical activity involves impact–like floor reaction forces [8]. In order to filter non–stationary signals, advanced filtering techniques like Discrete Wavelet Transforms [15], the Wigner Function [13] and Singular Spectrum Analysis [14] have been used.

Singular Spectrum Analysis (SSA) is a novel non–parametric technique used in the analysis of time series and based on principles of multivariate statistics. Its usefulness has been proven in the analysis of climatic, meteorological and geophysical time series [14]. A concise description of the method will be given in this section, whereas Golyandina et al. have presented a complete derivation [18].

The method starts by producing a Hankel matrix from the time series itself by sliding a window that is shorter in length than the original series. This step is referred to as "embedding". The columns of the matrix correspond to the terms inside the window for every position of said window. This matrix is then decomposed into a number of elementary matrices of decreasing norm. This step is called Singular Value Decomposition (SVD). Truncating the summation of elementary matrices yields an approximation of the original matrix. The approximation is one in which those elementary matrices that hardly contribute to the norm of the original matrix have been neglected. This step is called "grouping". Thus, the result is no longer a Hankel matrix, but an approximated time series may be recovered by taking the average of the diagonals. This new signal is the smoothed approximation of the original. This step is the "reconstruction" or the "diagonal averaging".

The above description may be put in formal terms as follows:

Step 1. Embedding

Let $\mathbf{F} = (f_0, f_1, \ldots, f_{N-1})$ be the length N time series representing the noisy signal. Let L be the window length, with $1 < L < N$ and L an integer. Each column $\mathbf{X}_j$ of the Hankel matrix corresponds to the "snapshot" taken by the sliding window: $\mathbf{X}_j = (f_{j-1}, f_j, \ldots, f_{j+L-2})^T, j = 1, 2, \ldots, K$, where $K = N - L + 1$ is the number of columns, that is, the number of different possible positions of said window. The matrix $\mathbf{X} = [\mathbf{X}_1, \mathbf{X}_2, \ldots, \mathbf{X}_K]$ is a Hankel matrix since all elements in diagonal $i + j = constant$ are equal. This matrix is sometimes referred to as the

trajectory matrix.

Step 2. Singular Value Decomposition (SVD) of the trajectory matrix.

It can be proven that the trajectory matrix (or any matrix, for that matter) may be expressed as the summation of d rank one elementary matrices $\mathbf{X} = \mathbf{E}_1 + \ldots + \mathbf{E}_d$, where d is the number of non-zero eigenvalues of the $L \times L$ matrix $\mathbf{S} = \mathbf{X} \cdot \mathbf{X^T}$. The elementary matrices are given by $\mathbf{E}_i = \sqrt{\lambda_i}\mathbf{U}_i\mathbf{V}_i^T$, $(i = 1, \ldots, d)$, where $\lambda_1, \ldots, \lambda_d$ are the non-zero eigenvalues of $\mathbf{S}$, in decreasing order,$\mathbf{U}_1, \ldots, \mathbf{U}_d$ are the corresponding eigenvectors, and vectors $\mathbf{V}_i$ are obtained from $\mathbf{V}_i = \mathbf{X^T} \cdot \mathbf{U}_i/\sqrt{\lambda_i}$, $i = 1, \ldots, d$

The norm of elementary matrix $\mathbf{E}_i$ equals $\sqrt{\lambda_i}$. Therefore, the contribution of the first matrices to the norm of $\mathbf{X}$ is much higher than the contribution of the last matrices. Therefore, it is likely that these last matrices represent noise in the signal. The plot of the eigenvalues in decreasing order is called the singular spectrum and is essential in deciding the index from where to truncate the summation.

Step 3. Grouping

This step is very simple when the method is used for smoothing a time series. It consist in approximating matrix $\mathbf{X}$ by the summation of the first r elementary matrices. In our case, matrix $\mathbf{X}$ is approximated by $\mathbf{X} \approx \mathbf{E}_1 + \mathbf{E}_2 + \ldots + \mathbf{E}_r$.

Step 4. Reconstruction (Diagonal Averaging)

The approximated matrix described above is no longer a Hankel matrix, but an approximated time series may be recovered by taking the average of the diagonals. Nevertheless, it may be more practical to carry out this averaging for each elementary matrix independently in order to obtain time series that represent the different components of the behavior of the original time series. These "elementary" time series are referred to as "principal components".

Let $\mathbf{Y}$ be any of the elementary matrices $\mathbf{E}_i$, the elements of which are y_{ij}, $1 \leq i \leq L$, $1 \leq j \leq K$. The time series $g_0, \ldots, g_{N-1}$ (principal component) corresponding to this elementary matrix is given by:

$$g_k = \begin{cases} \dfrac{1}{k+1} \displaystyle\sum_{m=1}^{k+1} y_{m,k-m+2} & \text{for } 0 \leq k < L^* - 1 \\ \dfrac{1}{L^*} \displaystyle\sum_{m=1}^{L^*} y_{m,k-m+2} & \text{for } L^* - 1 \leq k < K^* \\ \dfrac{1}{N-k} \displaystyle\sum_{m=k-K^*+2}^{N-K^*+1} y_{m,k-m+2} & \text{for } K^* \leq k < N \end{cases}$$

where $L^* = min(L, K)$, and $K^* = max(L, K)$. The smoothed time series is obtained by adding the first r principal components.

It is worth pointing out that the application of the basic SSA algorithm requires selecting the values of just two parameters: the window length L, and the number r of principal components to be retained in the reconstruction.

In order to demonstrate the performance of the SSA method, a non-stationary signal with impact taken from the biomechanical signal filtering literature [11] has been chosen. The signal is a measure of the angular coordinate of a pendulum impacting against a compliant wall [11, 13]. The angular acceleration obtained from the motion capture system is compared to that obtained directly (after dividing by pendulum length) from accelerometers. Three accelerometers were used in order to average their measurements to reduce noise. The average signal, logged at a sampling rate of 512 Hz is used as the acceleration reference signal.

Comparison with traditional filtering techniques is quantified by taking the root mean square of the error signal (RMSE) of displacement, velocity and acceleration. The error signal is the difference between the reference signal (or its derivatives) and the signal obtained after smoothing or filtering the raw data (or its derivatives). The result performing a double decomposition with $L_1, r_1 = (100, 9)$ and $L_2, r_2 = (20, 2)$ is RMSE = 23.04 rad/s2 (see Fig. 2). This result is similar to the value RMSE = 23.60 rad/s2 obtained by Giakas et al. (2000) with the help of the Wigner distribution and RMSE = 23.24 rad/s2 using generalized cross-validation quintic splines (GCVSPL).

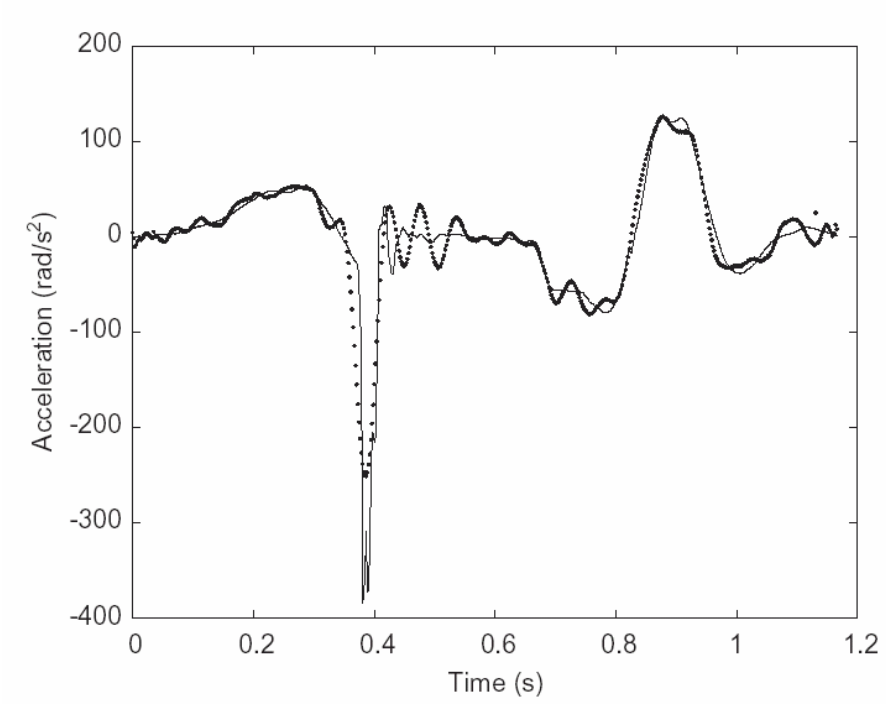

Figure 2: Reference angular acceleration (continuous line) and acceleration calculated from angular displacement data smoothed with a sequential SSA decomposition (dotted line).

4 RESULTS

To test the performance of the proposed procedure several raw displacement signals (observed signals) were processed using the smoothing procedure and the projection methods described in the previous sections. Two different kinematic data sets were used: computed generated data that simulate skin motion and experimental acquired data from a normal subject performing three different physical activities.

The results obtained by using the projection methods are compared with those obtained following the procedure proposed by Silva and Ambrósio [5].

4.1 Four-bar example

The computer generated data include the simulation of a four-bar crank-rocker mechanism during two crank revolutions (Fig. 3a). The input angular velocity and the lengths of the links were fixed to $\dot{\alpha} = 2\pi$ rad/s, $L_1 = 2$m, $L_2 = 8$m and $L_3 = 5$m. The time step is 0.01 seconds and the total time of simulation is 2 seconds.

The original data $\mathbf{q} = (x_1,\ y_1,\ x_2,\ y_2)^T$ were corrupted to simulate skin motion artifact and noise introduced by the motion capture system using three different patterns:

- Gaussian noise
- Sinusoidal stationary noise
- Non-stationary noise

The non-stationary noise is simulated by adding lumped point masses connected to the system by viscoelastic unions [8]. Figures 3c-3f show the original data and the corrupted data.

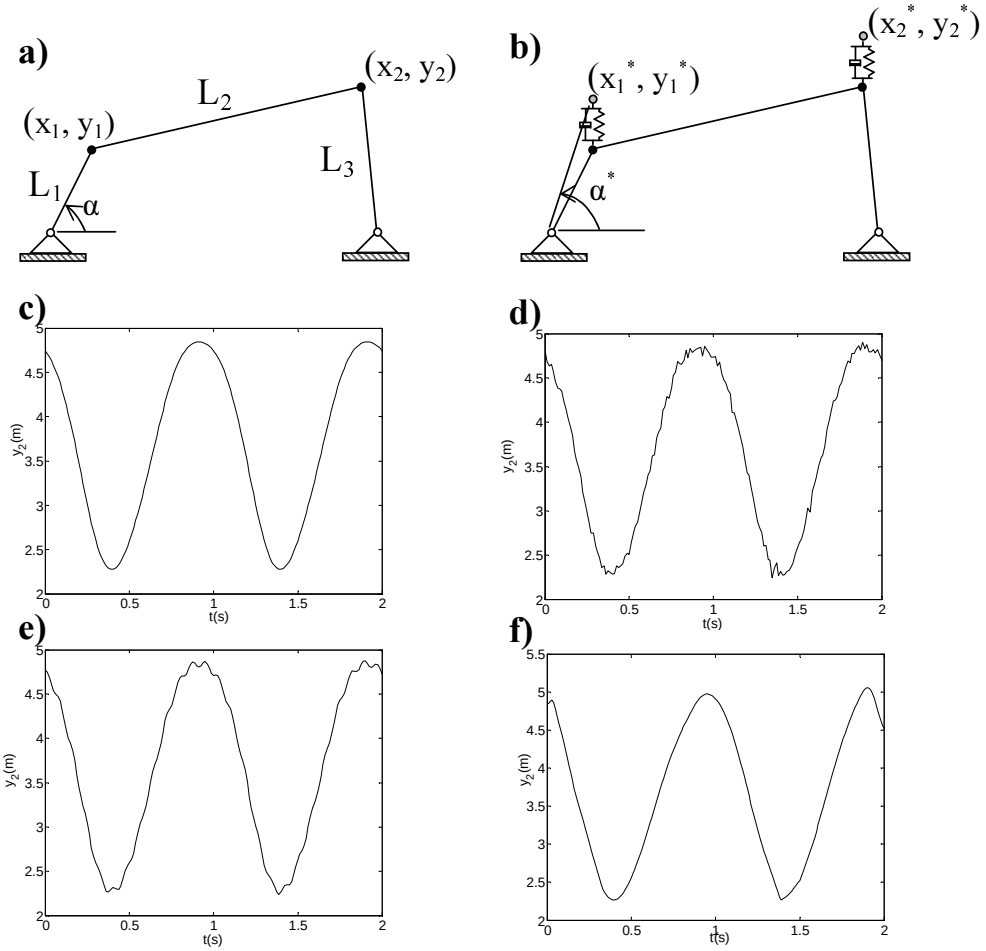

Figure 3: The four-bar example: a) original coordinates; b) model for the simulation of non-stationary noise; c) the original y_2; d) the corrupted y_2^* using Gaussian noise; e) the corrupted y_2^* using sinusoidal stationary noise; f) the corrupted y_2^* using non-stationary noise.

In order to compare the results obtained by different procedures we use the normalized root mean square (rms) of the residuals produced corresponding to the original coordinate q_i

$$\eta_i = \sqrt{\sum_{t=1}^{N} \left[q_i - q_i^*\right]^2 / \sum_{t=1}^{N} q_i^2} \tag{8}$$

$$\dot{\eta}_i = \sqrt{\sum_{t=1}^{N} \left[\dot{q}_i - \dot{q}_i^*\right]^2 / \sum_{t=1}^{N} \dot{q}_i^2} \tag{9}$$

$$\ddot{\eta}_i = \sqrt{\sum_{t=1}^{N} \left[\ddot{q}_i - \ddot{q}_i^*\right]^2 / \sum_{t=1}^{N} \ddot{q}_i^2} \tag{10}$$

Figure 4a shows the results obtained for the Gaussian noise (amplitude $p = 5L_1/100$) using the following procedures:

- Ensuring the kinematic consistency using the method proposed by Silva and Ambrósio [5] (KC)
- Using the projection methods for $\mathbf{q} = (x_1,\ y_1,\ x_2,\ y_2)^T$ and its higher derivatives (KCP).

Figure 4b shows the effect of the smoothing using the sequential SSA method with $L_1, r_1 = (20, 2)$, $L_2, r_2 = (20, 2)$ prior to the calculation of the higher derivatives.

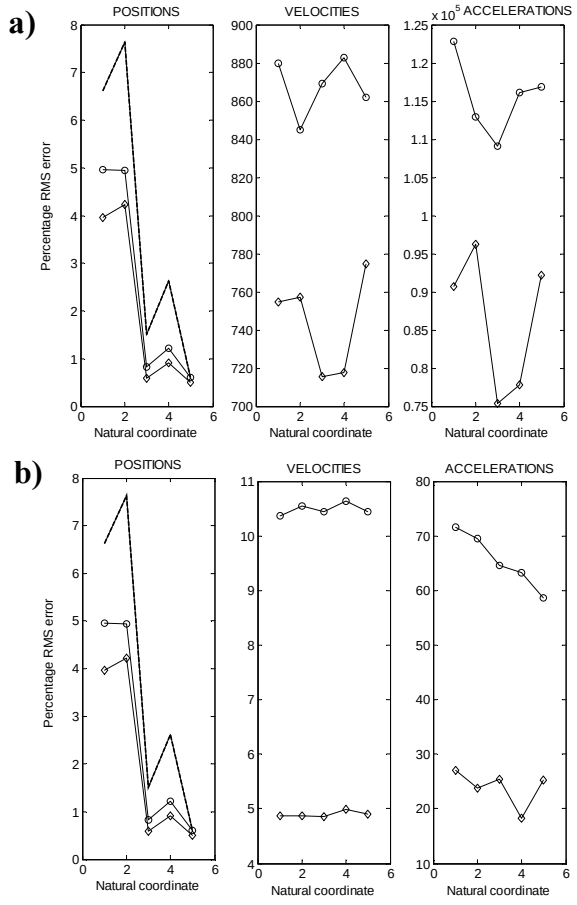

Figure 4: Residuals: a) no smoothing technique applied; b) SSA-smoothed signals. (o) KC, (⋄) KCP. The dashed line in the positions plots correspond to the corrupted data.

Figure 4 shows that the proposed projection process improves the results obtained by conventionally imposing kinematic consistency. Moreover, the smoothing of the angular displacement

Coordinate	$\mathbf{q}$	$\dot{\mathbf{q}}$	$\ddot{\mathbf{q}}$
RAW			
1	7.41 (**3.59**)	539.2 (**481.2**)	5502 (**3104**)
2	5.53 (**3.26**)	538.4 (**483.6**)	5255 (**2412**)
3	1.15 (**0.68**)	543.5 (**468.1**)	5546 (**2971**)
4	1.20 (**0.74**)	544.4 (**493.3**)	5699 (**2172**)
5	0.50 (**0.32**)	538.5 (**482.7**)	3387 (**2780**)
SSA			
1	7.41 (**3.59**)	10.55 (**8.51**)	63.18 (**26.88**)
2	5.53 (**3.26**)	9.26 (**7.26**)	54.65 (**24.75**)
3	1.15 (**0.68**)	9.38 (**6.91**)	58.00 (**25.56**)
4	1.20 (**0.74**)	10.42 (**8.38**)	53.36 (**18.80**)
5	0.50 (**0.32**)	8.18 (**5.73**)	43.31 (**25.74**)

Table 1: Summary of the results (Sinusoidal Stationary noise).

Coordinate	$\mathbf{q}$	$\dot{\mathbf{q}}$	$\ddot{\mathbf{q}}$
RAW			
1	1.46 (**1.35**)	526.9 (**489.7**)	6043 (**2870**)
2	1.33 (**1.32**)	526.6 (**488.1**)	5549 (**2518**)
3	0.23 (**0.22**)	528.2 (**488.8**)	4898 (**2725**)
4	0.31 (**0.27**)	531.9 (**501.6**)	4358 (**1911**)
5	0.17 (**0.16**)	526.4 (**492.8**)	4325 (**2710**)
SSA			
1	1.46 (**1.35**)	38.3 (**34.2**)	51.8 (**29.00**)
2	1.33 (**1.32**)	38.9 (**32.3**)	47.28 (**22.51**)
3	0.23 (**0.22**)	37.4 (**33.1**)	45.34 (**27.69**)
4	0.31 (**0.27**)	39.1 (**32.8**)	41.37 (**19.45**)
5	0.17 (**0.16**)	38.7 (**32.5**)	31.79 (**26.07**)

Table 2: Summary of the results (Non-stationary noise).

signal prior to differentiation dramatically improves the results. This fact illustrates the importance of the raw displacement smoothing and differentiation scheme in this problem. Tables 1 and 2 summarize results for the sinusoidal stationary noise and non-stationary noise using KC and KCP methods (boldface) using raw data to calculate higher derivatives (RAW) and smoothing the angular history using sequential SSA with $L_1, r_1 = (20, 2)$, $L_2, r_2 = (20, 2)$ prior to differentiation.

4.2 Biomechanical examples

In order to study the influence of the kinematic consistency procedure on the kinematics of a real biomechanical system three experimental data sets were acquired. The experimental data is the acquired motion of seven reflective markers placed on the right leg during:

- the impact phase of a drop landing from a height of 0.5 m.
- the impact phase of normal gait.

- the impact of normal running.

These activities have been chosen to study the influence of the degree of acceleration involved in the motion in the obtained results. Table 3 presents the experiment details. The layout of cameras and the set of points that were digitized are represented in Fig. 5.

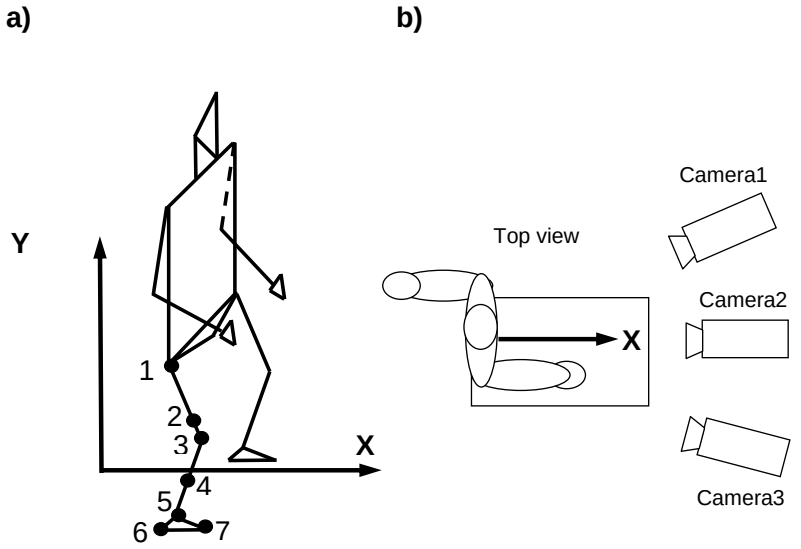

Figure 5: (a) Set of digitized points. (b) Layout of the biomechanics laboratory.

Characteristic	Description or Value
Motion capture system	Qualisys ProReflex MCU 200
Number of cameras	3
Sampling frequency (cameras)	200Hz
Simulation time	300 ms
Number of markers	7
Marker type	passive reflective

Table 3: Experimental system parameters.

The results obtained by using the projections procedure are compared with those obtained following the procedure proposed by Silva and Ambrósio [5]. The higher derivatives of the angular histories were calculated using the SSA scheme with $L, r = (20, 2)$ prior to differentiation with first-order finite differences. First, the initially non-consistent positions are used to calculate link lengths between the anatomical points. We select the initial link length (before impact) so that the model has constant link lengths during the analysis. Alternatively the direct measurement of the effective anthropometric dimensions of the subject under analysis can be used [5].

Different weighting factors in matrix $\mathbf{W}$ were assigned to each natural coordinate to reflect the average degree of skin movement artifact associated to each coordinate, namely the weighting factor for coordinate i was the coefficient of variation associated to that coordinate:

$$W_{ii} = \frac{\sigma_{q_i}}{\mu_{q_i}} \tag{11}$$

Where σ_{q_i} is the standard deviation of the coordinate and μ_{q_i} is the mean value of the coordinate q_i.

Figures 6-8 show the estimated vertical acceleration in the sagittal plane of markers 1 (great trochanter) and 3 (knee) for the impact phase. Several conclusion can be extracted from these figures:

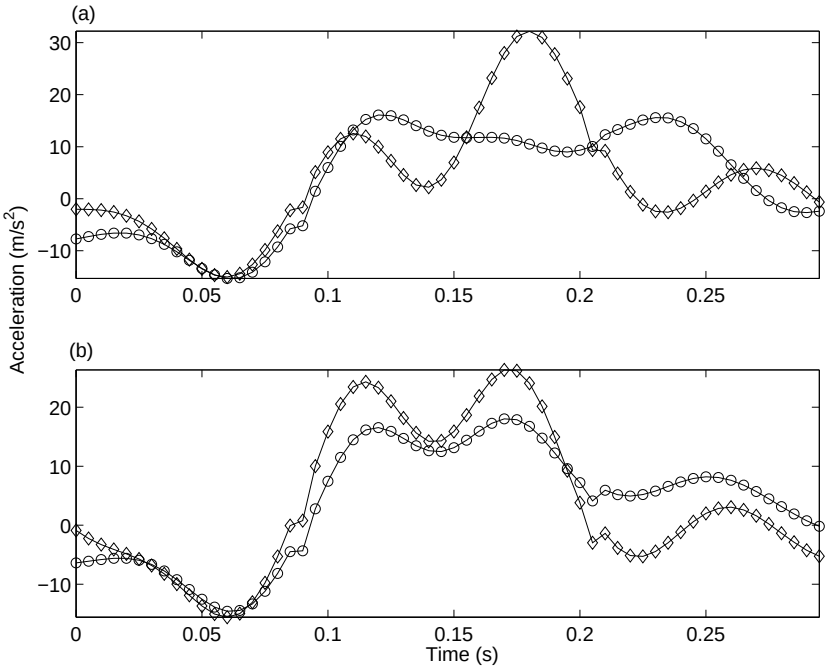

Figure 6: Estimated acceleration for the impact phase of a drop landing: a) Great trochanter (marker 1); b) Knee (marker 3). (o) KC, (◇) KCP.

- The two approaches produce similar results for the knee marker where the degree of skin motion is low (compare the Figs. 6-8b for the knee marker with figures 6-8a for the great trocanter marker where the skin motion is high).
- The major differences between the two methods occur in the neighborhood of the impact phase, that is, when the foot makes contact with the ground, at which instant the resulting jerk may be large. This divergence is higher for the Great trochanter marker than for the Knee marker in the three physical activities studied.

5 DISCUSSION AND CONCLUSIONS

A systematic multibody procedure based on orthogonal projection of the position, velocity and acceleration to the constraint manifold to ensure the kinematic data consistency in the context of the analysis of biomechanical systems is presented. The procedure corrects the marker positions and does not require intersegmental angles. Namely, the proposed scheme projects the subset of natural coordinates measured with the motion capture system and calculates the

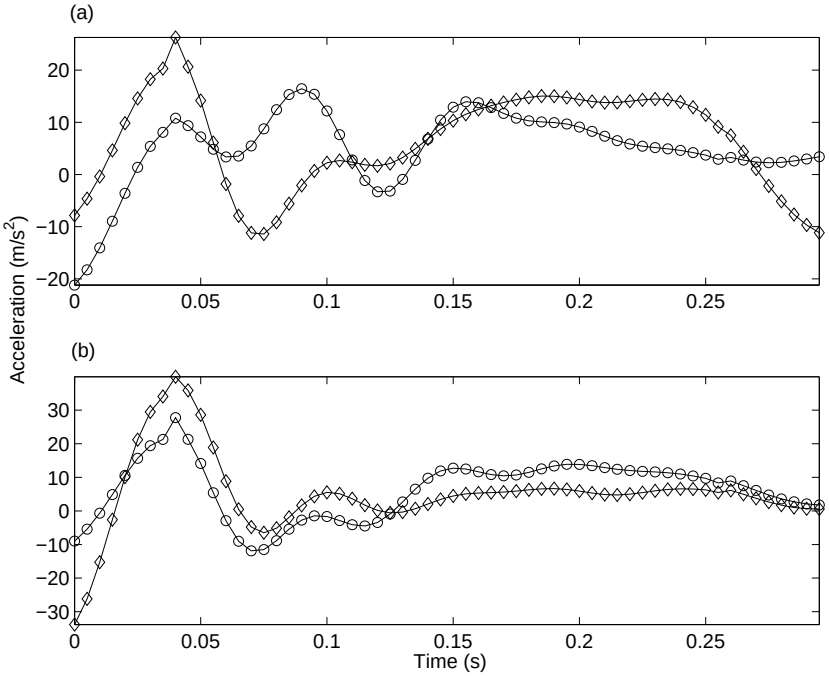

Figure 7: Estimated acceleration for the impact phase of running: a) Great trochanter (marker 1); b) Knee (marker 3). (o) KC, (◇) KCP.

angular histories from the consistent positions if required. Higher derivatives of consistent positions are then projected to the velocity and acceleration constraint manifold in order to obtain consistent velocities and accelerations.

Different weighting factors can be assigned to each natural coordinate to reflect the average degree of skin movement artifact associated to each coordinate. The improvement achieved by this technique with respect to other multibody based formalisms proposed in the literature is shown through the analysis of several examples that present simulated and measured skin motion artifacts and noise introduced by the motion capture system to study the influence of the most critical factors in this problem: kinematic consistency method and smoothing and differentiation procedures.

Future studies will focus on extending the projections of position velocity and acceleration equations to a large sample of subjects performing different physical activities, studying the variability of the results, and implementing an optimization scheme in the projection method in order to reproduce some observables produced by the real biosystem such us the ground reaction force. This fact is crucial to obtain a multibody model consistent with the acquired kinematic (kinematic consistency) and dynamic data (dynamic consistency). Another important objective to achieve is the integration of the smoothing and differentiation procedure in the projection scheme to perform the smoothing-derivation and projection to the constraint manifold in a single step.

REFERENCES

[1] H. Hatze. The fundamental problem of myoskeletal inverse dynamics and its implications *Journal of Biomechanics*, **35**, 109–115, 2002.

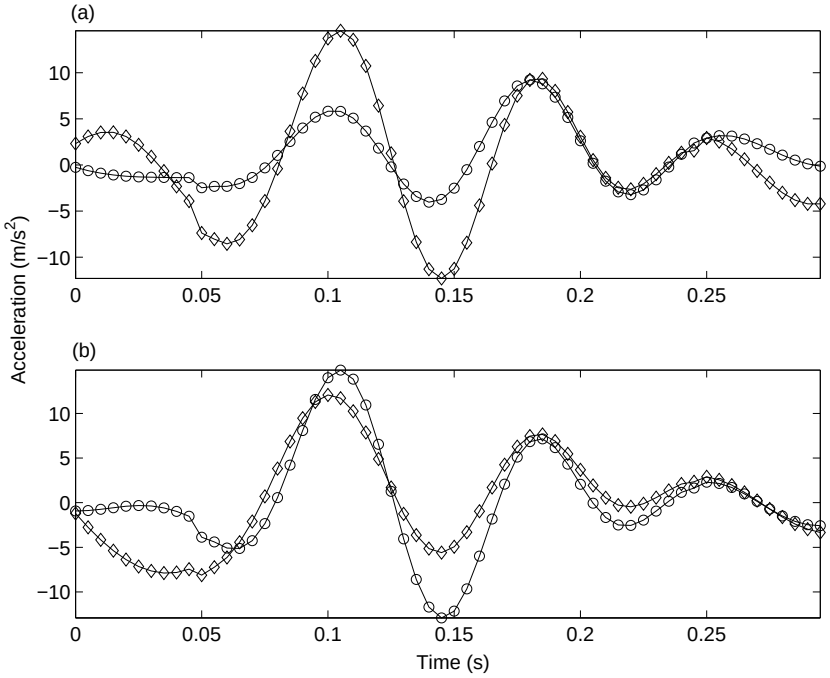

Figure 8: Estimated acceleration for the impact phase of walking: a) Great trochanter (marker 1); b) Knee (marker 3). (o) KC, (◇) KCP.

[2] A. Leardini, L. Chiari., U. Della Croce, A. Cappozzo. Human movement analysis using stereophotogrammetry Part 3. Soft tissue artifact assesment and compensation. *Gait and Posture*, **21**, 212–225, 2005.

[3] L. Chiari, U. Della Croce, A. Leardini, A. Cappozzo. Human movement analysis using stereophotogrammetry Part 2: Instrumental errors. *Gait and Posture*, **21**, 197–211, 2005.

[4] A. Capello, A. Capozzo, P.F: La Palombara, L. Luchetti, A. Leardini. Multiple anatomical landmark calibration for optimal bone pose estimation. *Human Movement Science*, **16**, 259–274, 1997.

[5] M.P.T. Silva, J.A.C. Ambrsio. Kinematic data consistency in the inverse dynamic analysis of biomechanical systems. *Multibody System Dynamics*, **8**, 219–239, 2002.

[6] E. Bayo, R. Ledesma. Augmented lagrangian and mass-orthogonal projection methods for constrained multibody dynamics. *Nonlinear Dynamics*, **9**, 113–130, 1996.

[7] J. Garcia de Jalon, E. Bayo. Kinematic and Dynamic Simulation of Multibody Systems. SpringerVerlag, Berlin/Heidelberg, 1994.

[8] T.W. Lu, J.J. O'Connor. Bone position estimation from skin marker co-ordinates using global optimisation with joint constraints. *Journal of Biomechanics*, **32**, 129–134, 1999.

[9] P. Cerveri, A. Pedotti., G. Ferrigno. Kinematical models to reduce the effect of skin artifacts on marker-based human motion estimation. *Journal of Biomechanics*, **38**, 2228–2236, 2005.

[10] C.L. Vaughan. Smoothing and differentiation of displacement-time data: an application of splines and digital filtering. *International Journal of Bio-Medical Computing*, **13**, 375–386, 1982.

[11] J. Dowling. A modelling strategy for the smoothing of biomechanical data. In: Johnsson, B. (Ed.), Biomechanics, Vol. XB. Human Kinetics, Champaign, IL, 1163-1167, 1985.

[12] G. Giakas, V. Baltzopoulos. Optimal digital filtering requires a different cut-off frequency strategy for the determination of the higher derivatives. *Journal of Biomechanics*, **30**, 851–855, 1997.

[13] G. Giakas, L.K. Stergioulas, A. Vourdas. Time-frequency analysis and filtering of kinematic signals with impacts using the Wigner function: accurate estimation of the second derivative. *Journal of Biomechanics*, **33**, 567–574, 2000.

[14] F. J. Alonso, J. M. Del Castillo, P. Pintado. Application of singular spectrum analysis to the smoothing of raw kinematic signals. *Journal of Biomechanics*, **38**, 1085–1092, 2005.

[15] R.I. Adham, S.A. Shihab. Discrete wavelet transform: a tool in smoothing kinematic data. *Journal of Biomechanics*, **32**, 317–321, 1999.

[16] F.J. Alonso, J.M. Del Castillo, P. Pintado. Motion data processing and wobbling mass modelling in the inverse dynamics of skeletal models. *Mechanism and Machine Theory*, in press, corrected-proof.

[17] M.P.T. Silva and J.A.C. Ambrósio, Sensitivity of the results produced by the inverse dynamic analisys of a human stride to perturbed input data, *Gait and Posture*, **19**, 35–49, 2004.

[18] N. Golyandina, V. Nekrutkin, A. Zhigljavsky. Analysis of Time Series Structure - SSA and Related Techniques. Chapman & Hall/CRC, Boca Raton, Florida, USA, 2001.